

## Methyl 4-O- $\beta$ -D-galactopyranosyl $\alpha$ -D-mannopyranoside methanol 0.375-solvate

Xiaosong Hu, Qingfeng Pan, Bruce C. Noll, Allen G. Oliver and Anthony S. Serianni\*

Department of Chemistry and Biochemistry, University of Notre Dame, Notre Dame, IN 46556-5670, USA

Correspondence e-mail: aseriann@nd.edu

Received 6 November 2009

Accepted 21 December 2009

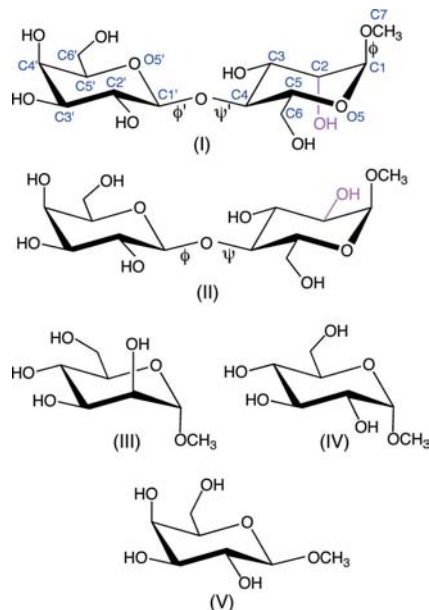
Online 15 January 2010

Methyl  $\beta$ -D-galactopyranosyl-(1 $\rightarrow$ 4)- $\alpha$ -D-mannopyranoside methanol 0.375-solvate,  $C_{13}H_{24}O_{11} \cdot 0.375CH_3OH$ , (I), was crystallized from a methanol-ethanol solvent system in a glycosidic linkage conformation, with  $\varphi'$  ( $O5_{Gal}-C1_{Gal}-O1_{Gal}-C4_{Man}$ ) =  $-68.2$  (3) $^\circ$  and  $\psi'$  ( $C1_{Gal}-O1_{Gal}-C4_{Man}-C5_{Man}$ ) =  $-123.9$  (2) $^\circ$ , where the ring is defined by atoms  $O5/C1-C5$  (monosaccharide numbering); C1 denotes the anomeric C atom and C6 the exocyclic hydroxymethyl C atom in the  $\beta Galp$  and  $\alpha Manp$  residues, respectively. The linkage conformation in (I) differs from that in crystalline methyl  $\alpha$ -lactoside [methyl  $\beta$ -D-galactopyranosyl-(1 $\rightarrow$ 4)- $\alpha$ -D-glucopyranoside], (II) [Pan, Noll & Serianni (2005). *Acta Cryst.* **C61**, o674–o677], where  $\varphi'$  is  $-93.6^\circ$  and  $\psi'$  is  $-144.8^\circ$ . An intermolecular hydrogen bond exists between  $O3_{Man}$  and  $O5_{Gal}$  in (I), similar to that between  $O3_{Glc}$  and  $O5_{Gal}$  in (II). The structures of (I) and (II) are also compared with those of their constituent residues, *viz.* methyl  $\alpha$ -D-mannopyranoside, methyl  $\alpha$ -D-glucopyranoside and methyl  $\beta$ -D-galactopyranoside, revealing significant differences in the Cremer–Pople puckering parameters, exocyclic hydroxymethyl group conformations and intermolecular hydrogen-bonding patterns.

### Comment

As a component of ongoing studies of the effects of primary structure and solvation on the conformations of biologically important oligosaccharides, the title disaccharide, methyl  $\beta$ -D-galactopyranosyl-(1 $\rightarrow$ 4)- $\alpha$ -D-mannopyranoside, (I), was prepared with  $^{13}C$ -enrichment at C1' and C4 to permit measurements of its constituent trans-glycoside  $J_{CH}$  and  $J_{CC}$  values (Bose *et al.*, 1998; Cloran *et al.*, 1999; Zhao *et al.*, 2008). These NMR parameters can be used to determine the preferred exocyclic C–O torsion angles,  $\varphi$  and  $\psi$ , comprising its internal glycosidic linkage. Compound (I) can be viewed as a derivative of methyl  $\alpha$ -lactoside [methyl  $\beta$ -D-galactopyranosyl-(1 $\rightarrow$ 4)- $\alpha$ -D-glucopyranoside], (II), the crystal structure of

which was reported recently (Pan *et al.*, 2005). A comparison of the structures of (I) and (II) in the crystalline and solution states allows an appraisal of the effect of the configuration at atom C2 on the conformation of the internal glycosidic linkage.



Disaccharide (I) (Fig. 1) was crystallized from a methanol-ethanol solvent system. The crystal structure of (I) is compared with that of (II), and with those of their respective constituent residues, *viz.* methyl  $\alpha$ -D-mannopyranoside, (III) (Jeffrey *et al.*, 1977), methyl  $\alpha$ -D-glucopyranoside, (IV) (Jeffrey *et al.*, 1977), and methyl  $\beta$ -D-galactopyranoside, (V) (Takagi & Jeffrey, 1979) (Table 1). In the following discussion, the quoted parameters are average values ( $\pm 1$  s.u.) across all indicated structures.

The endocyclic C–C bond lengths in (I)–(V) are similar [1.524 (6) Å for C1–C2 and 1.528 (7) Å for the remaining C–C bonds], showing that involvement of an anomeric C atom in an endocyclic C–C bond does not appreciably affect the length of the bond. In contrast, the average exocyclic C5–C6 bond length is 1.518 (3) Å, which is shorter than the average of the endocyclic C–C bond lengths.

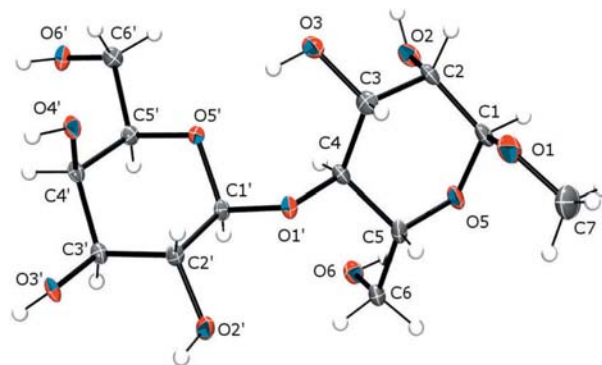


**Figure 1**  
The molecular structure of (I), showing the atom-numbering scheme. Displacement ellipsoids are drawn at the 50% probability level and H atoms are shown as small spheres of arbitrary radii.

The C—O bond lengths in (I)–(V) depend on structural context. Endocyclic C—O bonds (*i.e.* C1—O5 and C5—O5) are 1.428 (9) Å, and exocyclic C—O bonds are 1.421 (9) and 1.425 (9) Å for equatorial and axial bonds, respectively, that do not involve the anomeric C atom or other C atoms in a glycosidic linkage. The C1—O1 bond lengths are considerably shorter than other exo- and endocyclic C—O bonds and depend on bond orientation: axial 1.404 (5) Å and equatorial 1.389 (3) Å. The longer axial C1—O1 bond is presumably caused by  $n_{O5} \rightarrow \sigma^*_{C1}$  donation (anomeric effect; Lemieux, 1971). The remaining unique C—O bond, C4—O1', is elongated [1.446 (1) Å] in (I) and (II); the formation of the glycosidic linkage apparently introduces steric constraints that are relieved partly through lengthening of the C—O bond.

The internal glycosidic C1'—O1'—C4 bond angles in (I) and (II) [115.5 (3)°] are very similar, and both values are larger than the terminal C1—O1—C7 angles in (I)–(V) [113.5 (6)°].

The endocyclic torsion angles in both residues of (I) and (II) vary widely and indicate slight distortions from ideal  ${}^4C_1$  chair conformations. Cremer–Pople analysis (Cremer & Pople, 1975) showed relatively minor distortions in the  $\alpha$ Manp ( $\theta = 3.9^\circ$ ) and  $\alpha$ Glc p ( $\theta = 3.3^\circ$ ) rings of (I) and (II), respectively (Table 2). Intermediate distortion is observed in the  $\beta$ Galp ring of (I) ( $\theta = 6.5^\circ$ ), while the largest distortion is observed in the  $\beta$ Galp ring of (II) ( $\theta = 11.5^\circ$ ). The direction of distortion is similar for the  $\alpha$ Manp and  $\beta$ Galp residues of (I) and (II) ( $\varphi = 78 \pm 5^\circ$ ), indicating a  ${}^4C_1$  conformation slightly distorted towards  $B_{1,4}$  (atoms O5/C1—C5 define the saccharide ring; C1 is the anomeric C atom, C5 the final C atom around the ring and C6 is defined as the exocyclic hydroxymethyl C atom). The  $\alpha$ Glc p residue of (II) ( $\varphi = 105.0^\circ$ ) is distorted towards  ${}^5S_1$  (skew or twist-boat), while the  $\beta$ Galp residue of (I) ( $\varphi = 330.4^\circ$ ) is distorted towards  ${}^0S_2$ . Less distortion is observed in (III)–(V) than in the corresponding residues of the disaccharides. The directions of distortion in (III) and (IV) mimic those observed in the corresponding residues in the disaccharides. In contrast, the  $\beta$ Galp ring in (V) resembles that in (I), but not that in (II). These results show that the  $\beta$ Galp ring can deform considerably in disaccharides, and that the type of deformation varies widely even when the residues to which it is attached are similar. In the present case, the difference may be caused by the considerably different internal glycosidic linkage conformations (see below) and/or different crystal packing forces.

The internal glycosidic torsion angles,  $\varphi'$  and  $\psi'$ , in (I) differ considerably from the corresponding angles in (II) (Table 1). For  $\varphi'$  (O5'—C1'—O1'—C4), the difference is  $\sim 25^\circ$ , with the conformation about the C1'—O1' bond in (I) being closer to an ideal staggered geometry. For  $\psi'$  (C1'—O1'—C4—C5) the difference is  $\sim 21^\circ$ , with a nearly eclipsed conformation observed in (I). Interestingly, trans-glycoside  $J_{CH}$  and  $J_{CC}$  values (Bose *et al.*, 1998) in (I) and (II) have been shown recently to be identical (Hu, Pan & Serianni, unpublished results), suggesting that, in aqueous solution, both structures are likely to have identical linkage conformations. Apparently, crystal-packing forces in (I) stabilize the otherwise unfavorable linkage geometries expected from eclipsed interactions.

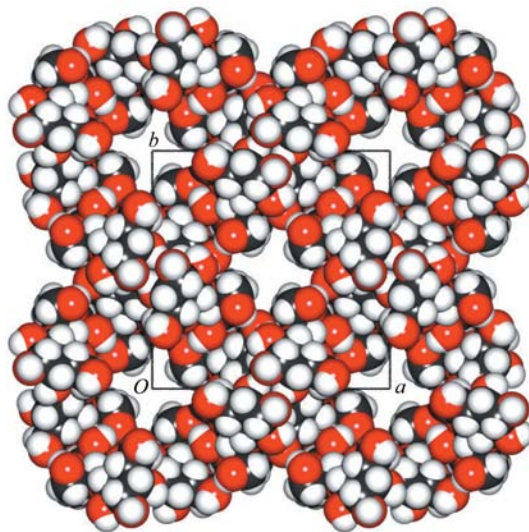


**Figure 2**  
A space-filling diagram of (I), viewed down the *c* axis.

The exocyclic hydroxymethyl (CH<sub>2</sub>OH) conformations in (I) and (II) differ significantly (Table 1). Torsion angles  $\omega$  (O5—C5—C6—O6) in the  $\alpha$ Manp and  $\alpha$ Glc p residues of (I) and (II) indicate *gg* and *gt* conformations, respectively. The *tg* conformation is found in the  $\beta$ Galp residue of (I), whereas *gt* is observed in the  $\beta$ Galp residue in (II). These observations are consistent with behavior found in solution by NMR, where a mix of *gg* and *gt* forms is commonly reported for  $\alpha$ Glc p and  $\alpha$ Manp rings, and a *gt/tg* mix is reported for  $\beta$ Galp (Thibaut *et al.*, 2004).

All hydroxy H atoms in (I) are involved as donors in intermolecular hydrogen bonding in the crystal structure, except that of O3, which is involved in an intramolecular hydrogen bond with atom O5'. All O atoms in (I) are involved in hydrogen bonding as mono-acceptors, except for O1, O2, O5 and O1'. Atoms O2', O3', O4', O6 and O6' are involved as mono-acceptors in intermolecular hydrogen bonding, and O5' serves as a mono-acceptor in an intramolecular hydrogen bond. In addition to serving as an intramolecular hydrogen-bond donor, atom O3 also serves as a mono-acceptor in an intermolecular hydrogen bond.

Like (I), all hydroxy H atoms in (II) are involved in intermolecular hydrogen bonding as donors, except that of O3 which participates in intramolecular hydrogen bonding to atom O5'. All O atoms, including O3, serve as mono-acceptors, except for O1, O5, O1' and O4', which are not hydrogen-bonded in the crystal structure. This pattern is similar, but not identical, to that observed in (I). Differences occur at O2 and O4'. Atom O2 serves as a hydrogen-bond acceptor but O4' does not in (II), whereas the opposite is observed in (I). These findings suggest that intermolecular hydrogen bonding to axial O atoms as acceptors may be more structurally demanding than for equatorial O atoms in saccharide crystal formation.

The symmetry adopted by the crystal packing (space group *I4*) results in a ring of hydrogen-bonded molecules about the

crystallographic fourfold *c* axis (Fig. 2 and Table 3). Furthermore, there are hydrogen bonds between molecules parallel to the *c* axis. This bonding results in channels running through the lattice parallel to the *c* axis. These channels are populated with diffuse disordered solvent that cannot be reliably modeled. Examination of a Fourier difference map shows that the electron density within this channel extends for the entire length of the unit cell. The arrangement of the disaccharides about the channel is such that the methyl group (C7) and the  $\beta$ Galp CH<sub>2</sub>OH functionality (C6') are oriented with their H atoms pointing towards the channel. Presumably this disposition renders the channel hydrophobic and this hydrophobicity may be the driving force for the presence of poorly located solvent molecule(s) within the channel. An analysis of the structure reveals a total of 390 Å<sup>-3</sup> of void space within

the unit cell. The electron count is 54 e<sup>-</sup>. See *Refinement* section for further details.

## Experimental

The crystal structure of (I) was determined using a <sup>13</sup>C-labeled form of the molecule, which was prepared according to a seven-step procedure (see supplementary material).

Compound (XII) (0.64 g, 0.81 mmol) was dissolved in methanol (20 ml) and treated with a small amount of sodium methoxide (until the pH of the solution reached ~10) at room temperature for 3 h, and then neutralized with Dowex 50 × 8 (200–400 mesh) (H<sup>+</sup>) ion-exchange resin. The resulting solution was filtered, and the filtrate was evaporated to dryness. The residue was dissolved in ethanol (20 ml) and treated with Pd/C (0.22 g) and H<sub>2</sub> overnight to afford

**Table 1**

Comparison of structural parameters (Å, °) for (I)–(V).

Compound (I) is methyl  $\beta$ -Gal- $\alpha$ -Man, (II) is methyl  $\beta$ -Gal- $\alpha$ -Glc, (III) is methyl  $\alpha$ -Man, (IV) is methyl  $\alpha$ -Glc and (V) is methyl  $\beta$ -Gal. *gt* is *gauche-trans*, *gg* is *gauche-gauche* and *tg* is *trans-gauche*.

Parameter	(I)	(II)	(III)	(IV)	(V)
<b>Bond lengths</b>					
C1–C2	1.520 (4)	1.5268 (19)	1.524 (1)	1.528 (2)	
C2–C3	1.520 (4)	1.5221 (19)	1.529 (1)	1.521 (2)	
C3–C4	1.517 (4)	1.5295 (17)	1.520 (1)	1.532 (2)	
C4–C5	1.528 (5)	1.5296 (18)	1.529 (1)	1.530 (2)	
C5–C6	1.521 (4)	1.5159 (18)	1.519 (1)	1.515 (2)	
C1'–C2'	1.514 (4)	1.5316 (17)			1.526 (2)
C2'–C3'	1.523 (4)	1.5437 (17)			1.523 (2)
C3'–C4'	1.530 (4)	1.5432 (19)			1.523 (2)
C4'–C5'	1.537 (4)	1.5325 (18)			1.529 (2)
C5'–C6'	1.521 (4)	1.5183 (18)			1.515 (2)
C1–O1	1.412 (4)	1.4012 (19)	1.401 (2)	1.401 (3)	
C1–O5	1.418 (4)	1.4156 (15)	1.415 (2)	1.414 (3)	
C2–O2	1.420 (3)	1.4185 (15)	1.415 (2)	1.410 (3)	
C3–O3	1.437 (4)	1.4329 (16)	1.422 (2)	1.420 (3)	
C4–O4			1.429 (2)	1.414 (3)	
C5–O5	1.434 (3)	1.4364 (17)	1.439 (2)	1.428 (3)	
C6–O6	1.419 (4)	1.4317 (16)	1.413 (2)	1.421 (3)	
C1'–O1'	1.391 (3)	1.3857 (14)			1.389 (2)
C1'–O5'	1.429 (3)	1.4295 (16)			1.425 (2)
C2'–O2'	1.405 (3)	1.4225 (16)			1.424 (2)
C3'–O3'	1.428 (3)	1.4219 (15)			1.414 (2)
C4'–O4'	1.438 (3)	1.4273 (18)			1.426 (2)
C5'–O5'	1.433 (3)	1.4397 (15)			1.430 (2)
C6'–O6'	1.426 (3)	1.4333 (17)			1.418 (3)
C4–O1'	1.445 (3)	1.4467 (17)			
O3...O5'	2.76	2.82			
<b>Bond angles</b>					
C1'–O1'–C4	115.7 (2)	115.26 (10)			
C1–O1–C7	114.0 (3)	112.66 (14)	113.9 (1)	113.8 (1)	113.2
O3–O3H–O5'	161	151			
<b>Torsion angles</b>					
C1–C2–C3–C4	–53.7 (3)	–54.6	–53.4 (1)	–55.3 (1)	
C1'–C2'–C3'–C4'	–51.2 (3)	–57.6			–51.0 (2)
C1–O5–C5–C4	56.7 (3)	56.6	59.1 (1)	58.4 (1)	
C1'–O5'–C5'–C4'	66.4 (2)	59.6			65.4 (2)
C2–C1–O1–C7 ( $\varphi$ )	–174.5 (2)	–165.5	–177.7 (1)	–175.2 (1)	
O5–C1–O1–C7 ( $\varphi$ )	64.3 (3)	72.6	60.5 (1)	62.7 (1)	
C2'–C1'–O1'–C4 ( $\varphi'$ )	173.1 (2)	148.1			163.3 (2)
O5'–C1'–O1'–C4 ( $\varphi'$ )	–68.2 (3)	–93.6			–77.1 (2)
C1'–O1'–C4–C3 ( $\psi'$ )	115.2 (2)	93.6			
C1'–O1'–C4–C5 ( $\psi'$ )	–123.9 (2)	–144.8			
H1'–C1'–O1'–C4 ( $\varphi'$ )	53	26			
C1'–O1'–C4–H4 ( $\psi'$ )	–4	–28			
O5–C5–C6–O6 ( $\omega$ )	–63.8 (3) ( <i>gg</i> )	72.6 ( <i>gt</i> )	–65.1 (1) ( <i>gg</i> )	74.0 (1) ( <i>gt</i> )	
O5'–C5'–C6'–O6' ( $\omega'$ )	160.7 (2) ( <i>tg</i> )	69.2 ( <i>gt</i> )			63.5 (2) ( <i>gt</i> )

**Table 2**

Cremer–Pople puckering parameters for (I)–(V).

Compound	Ring	$Q$ (Å)	$\varphi$ (°)	$\theta$ (°)
(I)	$\beta$ Galp	0.5957	330.4	6.5
	$\alpha$ Manp	0.5527	81.7	3.9
(II)	$\beta$ Galp	0.6048	74.4	11.5
	$\alpha$ GlcP	0.5575	105.0	3.3
(III)	$\alpha$ Manp	0.5565	46.1	0.5
(IV)	$\alpha$ GlcP	0.5694	116.7	2.2
(V)	$\beta$ Galp	0.5827	346.2	5.9

**Table 3**

Hydrogen-bond geometry for (I) (Å, °).

$D-H\cdots A$	$D-H$	$H\cdots A$	$D\cdots A$	$D-H\cdots A$
$O2-H2\cdots O6^i$	0.84	2.08	2.839 (3)	151
$O3-H3\cdots O5^i$	0.84	1.95	2.755 (3)	161
$O6-H6\cdots O6^i$	0.84	1.94	2.771 (3)	170
$O2'-H2'\cdots O3^{ii}$	0.84	1.82	2.636 (3)	163
$O3'-H3'\cdots O4^{iii}$	0.84	2.05	2.885 (3)	171
$O4'-H4'\cdots O3^{iii}$	0.84	2.05	2.884 (3)	173
$O6'-H6'\cdots O2^{iv}$	0.84	2.14	2.843 (3)	142
$O6'-H6'\cdots O1^{iv}$	0.84	2.38	3.108 (3)	145

Symmetry codes: (i)  $-x + \frac{1}{2}, -y + \frac{1}{2}, z - \frac{1}{2}$ ; (ii)  $-y + \frac{1}{2}, x + \frac{1}{2}, z + \frac{1}{2}$ ; (iii)  $-x, -y + 1, z$ ; (iv)  $y - \frac{1}{2}, -x + \frac{1}{2}, z + \frac{1}{2}$ .

methyl 4-*O*- $\beta$ -D-[1-<sup>13</sup>C]galactopyranosyl- $\alpha$ -D-[4-<sup>13</sup>C]mannopyranoside, (I). Purification by crystallization from a slowly cooled 2:1 methanol–ethanol solution gave (I) (0.25 g, 0.75 mmol, ~93%).

*Crystal data*

$C_{13}H_{24}O_{11} \cdot 0.375CH_4O$   $Z = 8$   
 $M_r = 368.34$  Cu  $K\alpha$  radiation  
 Tetragonal,  $I4$   $\mu = 1.09 \text{ mm}^{-1}$   
 $a = 20.1789$  (4) Å  $T = 100 \text{ K}$   
 $c = 8.4712$  (2) Å  $0.25 \times 0.05 \times 0.05 \text{ mm}$   
 $V = 3449.37$  (13) Å<sup>3</sup>

*Data collection*

Bruker APEX diffractometer 12483 measured reflections  
 Absorption correction: empirical 2783 independent reflections  
 (using intensity measurements) 2650 reflections with  $I > 2\sigma(I)$   
 (SADABS; Sheldrick, 2003)  $R_{int} = 0.036$   
 $T_{min} = 0.776, T_{max} = 0.949$

*Refinement*

$R[F^2 > 2\sigma(F^2)] = 0.044$  H-atom parameters constrained  
 $wR(F^2) = 0.104$   $\Delta\rho_{max} = 0.44 \text{ e } \text{Å}^{-3}$   
 $S = 1.12$   $\Delta\rho_{min} = -0.26 \text{ e } \text{Å}^{-3}$   
 2783 reflections Absolute structure: Flack (1983),  
 218 parameters with 1495 Friedel pairs  
 1 restraint Flack parameter: 0.0 (2)

The absolute configuration of (I) was determined by a comparison of the intensities of Friedel pairs of reflections and by the known handedness of the precursor molecules. Both techniques agreed and the correct absolute configuration is depicted. Hydroxy group H

atoms were located in a difference Fourier map, but were included in riding positions best defined to reduce the electron density at that location ( $O-H = 0.84 \text{ Å}$ ). All other H atoms were included in calculated positions ( $C-H = 0.98-1.00 \text{ Å}$ ).  $U_{iso}(H) = 1.5U_{eq}(C)$  for methyl H or  $1.2U_{eq}(C,O)$  for all other H atoms.

The SQUEEZE routine from PLATON (Spek, 2009) was applied to the data to account for the solvent void within the lattice. Two void spaces with a total void volume of  $390 \text{ Å}^{-3}$  and a sum of  $54 e^-$  were accounted for within the unit cell. This could be accounted for by the inclusion of three molecules of methanol per unit cell. Thus, three molecules of methanol were included per unit cell (0.375 per formula unit) for the purposes of calculating  $\mu, \rho, F(000)$ , etc. Examination of the electron density within this pore shows an elongated tube of ill-defined density.

Data collection: APEX2 (Bruker–Nonius, 2008); cell refinement: APEX2 and SAINT (Bruker–Nonius, 2008); data reduction: SAINT and XPREP (Sheldrick, 2008); program(s) used to solve structure: SHELXS97 (Sheldrick, 2008); program(s) used to refine structure: SHELXL97 (Sheldrick, 2008); molecular graphics: XP in SHELXTL (Sheldrick, 2008), POV-RAY (Version 3.6.2; Cason, 2003) and DIAMOND (Version 3.2c; Brandenburg, 2009); software used to prepare material for publication: XCIF (Sheldrick, 2008), enCIFer (Allen et al., 2004) and publCIF (Westrip, 2010).

Supplementary data for this paper are available from the IUCr electronic archives (Reference: GZ3172). Services for accessing these data are described at the back of the journal.

**References**

Allen, F. H., Johnson, O., Shields, G. P., Smith, B. R. & Towler, M. (2004). *J. Appl. Cryst.* **37**, 335–338.  
 Austin, P. W., Hardy, F. E., Buchanan, J. G. & Baddiley, J. (1963). *J. Chem. Soc.* pp. 5350–5353.  
 Bose, B., Zhao, S., Stenutz, R., Cloran, F., Bondo, P. B., Bondo, G., Hertz, B., Carmichael, I. & Serianni, A. S. (1998). *J. Am. Chem. Soc.* **120**, 11158–11173.  
 Brandenburg, K. (2009). *DIAMOND*. Crystal Impact GbR, Bonn, Germany.  
 Bruker–Nonius (2008). *APEX2* and *SAINTE*. Bruker–Nonius AXS Inc., Madison, Wisconsin, USA.  
 Cason, C. J. (2003). *POV-RAY*. Persistence of Vision Raytracer Pty. Ltd, Victoria, Australia.  
 Cloran, F., Carmichael, I. & Serianni, A. S. (1999). *J. Am. Chem. Soc.* **121**, 9843–9851.  
 Cremer, D. & Pople, J. A. (1975). *J. Am. Chem. Soc.* **97**, 1354–1358.  
 Flack, H. D. (1983). *Acta Cryst.* **A39**, 876–881.  
 Jeffrey, G. A., McMullan, R. K. & Takagi, S. (1977). *Acta Cryst.* **B33**, 728–737.  
 Lemieux, R. U. (1971). *Pure Appl. Chem.* **25**, 527–548.  
 Pan, Q., Noll, B. C. & Serianni, A. S. (2005). *Acta Cryst.* **C61**, o674–o677.  
 Schmidt, R. R. (1986). *Angew. Chem. Int. Ed. Engl.* **25**, 212–235.  
 Sheldrick, G. M. (2003). *SADABS*. University of Göttingen, Germany.  
 Sheldrick, G. M. (2008). *Acta Cryst.* **A64**, 112–122.  
 Spek, A. L. (2009). *Acta Cryst.* **D65**, 148–155.  
 Takagi, S. & Jeffrey, G. A. (1979). *Acta Cryst.* **B35**, 902–906.  
 Thibaudeau, C., Stenutz, R., Hertz, B., Klepach, T. E., Zhao, S., Wu, Q., Carmichael, I. & Serianni, A. S. (2004). *J. Am. Chem. Soc.* **126**, 15668–15685.  
 Westrip, S. P. (2010). *publCIF*. In preparation.  
 Yamazaki, F., Sato, S., Nukada, T., Ito, Y. & Ogawa, T. (1990). *Carbohydr. Res.* **201**, 31–50.  
 Zhao, H., Carmichael, I. & Serianni, A. S. (2008). *J. Org. Chem.* **73**, 3255–3257.